JOC Article

Enhanced Diastereoselectivity via Confinement: Photoisomerization of 2,3-Diphenylcyclopropane-1-carboxylic Acid Derivatives within Zeolites

J. Sivaguru,[†] Raghavan. B. Sunoj,[‡] Takehiko Wada,[§] Yumi Origane,[||] Yoshihisa Inoue,[§,||] and Vaidhyanathan Ramamurthy*,[†]

Department of Chemistry, Tulane University, New Orleans, Louisiana 70118, Department of Chemistry, Indian Institute of Technology, Bombay, Mumbai 400076, India, Department of Molecular Chemistry and PRESTO (JST), Osaka University, 2-1 Yamada-oka, Suita 565-0871, Japan, and ICORP Entropy Control Project, JST, 4-6-3 Kamishinden, Toyonaka 560-0085, Japan

murthy@tulane.edu

Received April 15, 2004

From the perspective of asymmetric induction, the photochemistry of 24 chiral esters and amides of *cis*-2,3-diphenylcyclopropane-1-carboxylic acid from excited singlet and triplet states has been investigated within zeolites. The chiral auxiliaries placed at a remote location from the isomerization site functioned far better within a zeolite than in solution. Generally, chiral auxiliaries with an aromatic or a carbonyl substituent performed better than the ones containing only alkyl substituents. A model based on cation-binding-dependent flexibility of the chiral auxiliary accounts for the observed variation in de between aryl (and carbonyl) and alkyl chiral auxiliaries within zeolites. Cation-dependent diastereomer switch was also observed in select examples.

Introduction

Following the communication by Hammond and Cole in 1965 on the photosensitized isomerization of *cis*-diphenylcyclopropane,[1] several groups have performed enantio- and diastereoselective phototransformations both in solution[2] and in the solid state.[3] In solution, despite considerable efforts, the enantiomeric excess (ee) obtained under ambient conditions continues to be less than 50%. The best results in solution have been obtained via the chiral auxiliary methodology[4] yielding in select examples diastereomeric excess (de) close to 100%. Unfortunately, the generality of this approach is yet to be established.

Asymmetric photochemistry in the crystalline state is based on "chance" crystallization of achiral molecules in a chiral space group.[3a,b] Because of its limited probability, there are only very few examples of asymmetric induction during photolysis of achiral molecules in the crystalline state. A more general methodology known as the "ionic chiral auxiliary approach" introduced by Scheffer facilitated achiral molecules to crystallize in a chiral space group.[3c] This approach is limited to molecules with carboxylic acid groups that form crystallizable salts with chiral amines or vice versa. Recognizing the problem of crystallizing achiral molecules in a chiral space group, several researchers have explored chiral hosts as the reaction medium.[3d] The success of this approach is limited to guests that can form solid solutions with the host without disturbing the host's macrostructure. The reactivity of molecules in the crystalline state and in solid host−guest assemblies is controlled by the details of molecular packing. Currently, molecular packing and consequently the chemical reactivity in the crystalline state cannot be reliably predicted. Therefore, even after successfully crystallizing a molecule in a chiral space group or complexing a molecule with a chiral host or a chiral auxiliary, there is no guarantee that the guest will react in the crystalline state. Hence, even though crystalline and host−guest assemblies have been very useful in conducting enantioselective photoreactions, their general applicability thus far has been limited.

We believe that zeolites offer a solution to the above limitations. For example, guest molecules present within zeolites possess greater freedom than in crystals/solid host−guest assemblies and less freedom than in isotropic solvents. This permits molecules within zeolites to react more freely than in crystals/solid host−guest assemblies

[†] Tulane University.
[‡] Indian Institute of Technology.
[§] Osaka University.
[||] ICORP Entropy Control Project.

(1) Hammond, G. S.; Cole, R. S. *J. Am. Chem. Soc.* **1965**, *87*, 3256.
(2) (a) Inoue, Y. *Chem. Rev.* **1992**, *92*, 741. (b) Rau, H. *Chem. Rev.* **1983**, *83*, 535−547. (c) Laarhoven, W. H.; Cuppen, T. J. H. M. *J. Chem. Soc., Chem. Commun.* **1977**, 47. (d) Laarhoven, W. H.; Cuppen, T. J. H. M. *J. Chem. Soc., Perkin Trans. 2* **1978**, 315−318. (e) Balavoine, G.; Moradpour, A.; Kagan, H. B. *J. Am. Chem. Soc.* **1974**, *96*, 5152. (f) Zandomeneghi, M.; Cavazza, M.; Pietra, F. *J. Am. Chem. Soc.* **1984**, *106*, 7261−7262. (g) Moradpour, A.; Kagan, H.; Baes, M.; Morren, G.; Martin, R. H. *Tetrahedron* **1975**, *31*, 2139. (h) Tsuneishi, H.; Hakushi, T.; Inoue, Y. *J. Chem. Soc., Perkin Trans. 2* **1996**, 1601−1605. (i) Inoue, Y.; Wada, T.; Asaoka, S.; Sato, H.; Pete, J.-P. *J. Chem. Soc., Chem. Commun.* **2000**, 251−259.
(3) (a) Vaida, M.; Popovitz-Biro, R.; Leserowitz, L.; Lahav., M. In *Photochemistry in Organized and Constrained Media*; Ramamurthy, V., Ed.; VCH: New York, 1991; pp 247−302. (b) Evans, S. V.; Garcia-Garibay, M.; Omkaram, N.; Scheffer, J. R.; Trotter, J.; Wireko, F. *J. Am. Chem. Soc.* **1986**, *108*, 5648−5650. (c) Leibovitch, M.; Olovsson, G., Scheffer, J. R.; Trotter, J. *Pure Appl. Chem.* **1997**, *67*, 815−823. (d) Toda, F. *Acc. Chem. Res.* **1995**, *28*, 480. (e) Tanaka, K.; Fujiwara, T.; Urbanczyk-Lipkowska, Z. *Org. Lett.* **2002**, *4*, 3255−3257.
(4) (a) Nehrings, A.; Scharf, H. D.; Runsink, J. *Angew. Chem.* **1985**, *97*, 882−883. (b) Inoue, T.; Matsuyama, K.; Inoue, Y. *J. Am. Chem. Soc.* **1999**, *121*, 9877.

10.1021/jo049365i CCC: $27.50
Published on Web 08/31/2004

SCHEME 1

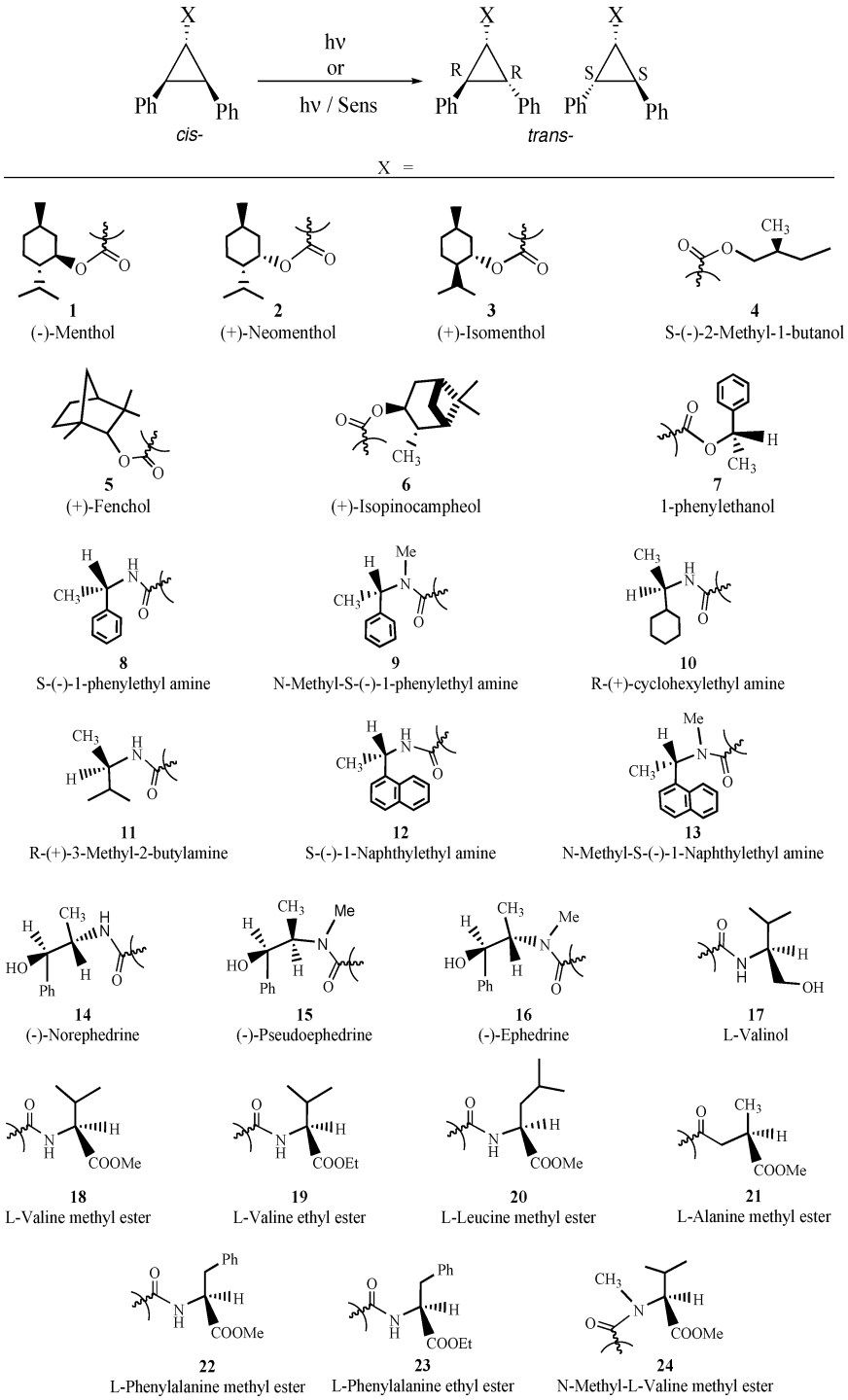

and more selectively than in solutions. Zeolites, unlike organic host systems, can include a large number of molecules, with the only limitation being that the dimensions of the guest be less than the pore dimensions of the zeolite.[5] A variety of molecules can therefore be included within a zeolite and induced to react. A major deficiency is that the zeolite is not chiral. To provide the asymmetric environment lacking in zeolites during the reaction, a chiral source had to be employed. For this purpose, in the approach we refer to as the "chiral inductor method", where optically pure chiral inductors such as ephedrine were used, the nonchiral surface of the zeolite becomes "locally chiral" in the presence of a chiral inductor.[6] This approach gave close to 15% ee with several achiral *cis*-2,3-diphenylcyclopropane-1-carboxylic acid derivatives in the presence of chiral inductors such

(5) (a) Ramamurthy, V. In *Photochemistry in Organized and Constrained media*; Ramamurthy, V., Ed.; VCH: New York, 1991; p 429. (b) Breck, D. W. *Zeolite Molecular Sieves, Structure, Chemistry and Use*; John Wiley & Sons: New York, 1974. (c) Dyer, A. *An introduction to zeolite molecular sieves*; John Wiley & Sons: New York, 1988. (d) Meier, W. M.; Olson, D. H. *Atlas of Zeolite Structure Types*, 3rd ed.; Butterworth-Heinemann: London, 1992.

SCHEME 2

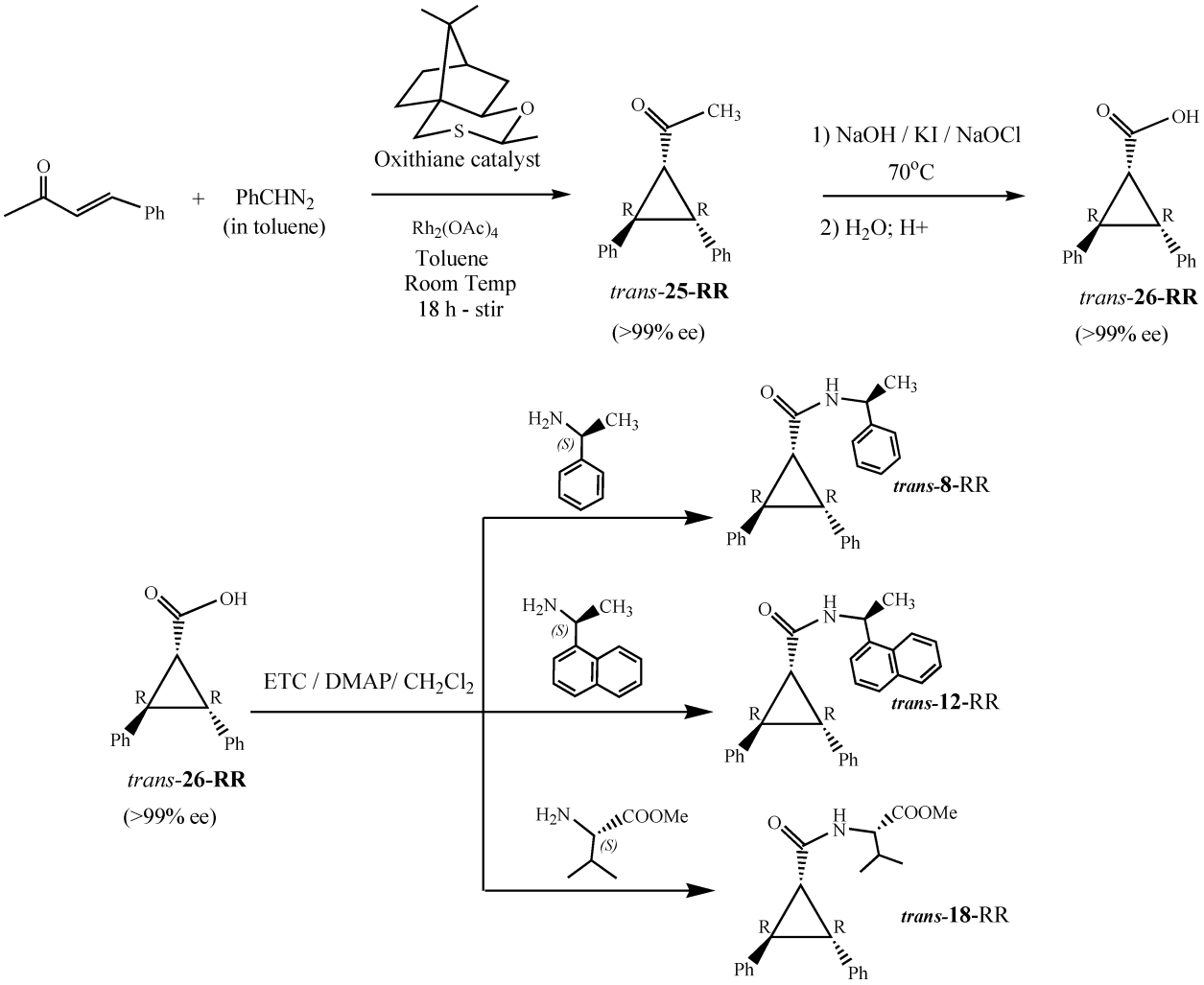

as optically pure 1-cyclohexylethylamine, pseudoephedrine, and norephedrine.[7] Therefore, we have explored a different strategy termed the "chiral auxiliary method" in which the chiral perturber is connected to the reactant via a covalent bond. We envisioned that a confined space offered by a zeolite would augment the influence of a chiral auxiliary.[6,8] It is gratifying to observe that this has been the case during the photoisomerization from S_1 and T_1 of a number of *cis*-2,3-diphenylcyclopropane-1-carboxylic acid derivatives within alkali ion exchanged Y zeolites.[8a,9] The systems investigated and the products of photoreactions are listed in Scheme 1. Chiral perturbers were internally built into the reactants such that it is present at a slightly remote location from the reaction site. As discussed in this paper, these remotely located chiral perturbers function much more effectively within a zeolite than in an organic solvent medium. In this process, alkali ions present within a zeolite play a crucial role.

Results

To explore the role of constrained environment (zeolite) on the asymmetric induction during the geometric isomerization of *cis*- to *trans*-diphenylcyclopropane, a detailed photochemical study of *cis*-2,3-diphenylcyclopropane-1-carboxylic acid derivatives affixed with chiral auxiliaries (24 compounds in total) was undertaken. The results of these studies are presented in this section.

The stereoisomers (*RR*- and *SS*-isomers) of *trans*-**8** were obtained in pure form by preparative HPLC (Chiralcel OD column). The absolute configuration of the isolated isomers was assigned by matching their chiral GC/HPLC retention times with those of pure isomers synthesized as outlined in the Supporting Information. (2*R*,3*R*)-1-Acetyl-2,3-diphenylcyclopropane **25** synthesized by a procedure reported by Aggarwal and co-workers[10,11] (Scheme 2) was used as the precursor for *trans*-**26**-*RR*.

(6) (a) Sivaguru, J.; Natarajan, A.; Kaanumalle, L. S.; Shailaja, J.; Uppili, S.; Joy, A.; Ramamurthy, V. *Acc. Chem. Res.* **2003**, *36*, 509−521. (b) Sivaguru, J.; Shailaja, J.; Uppili, S.; Ponchot, K.; Joy, A.; Arunkumar, N.; Ramamurthy, V. In *Organic Solid State Reactions*; Toda, F., Ed.; Kluwer Academic Press: Dordrecht, The Netherlands, 2002; pp 159−188. (c) Joy, A.; Ramamurthy, V. *Chem. Eur. J.* **2000**, *6*, 1287−1293.

(7) (a) Cheung, E.; Chong, K. C. W.; Jayaraman, S.; Ramamurthy, V.; Scheffer, J. R.; Trotter, J. *Org. Lett.* **2000**, *2*, 2801−2804. (b) Kaanumalle, L. S.; Sivaguru, J.; Sunoj, R. B.; Lakshminarasimhan, P.; Chandrasekhar, J.; Ramamurthy, V. *J. Org. Chem.* **2002**, *67*, 8711−8720.

(8) (a) Sivaguru, J.; Scheffer, J. R.; Chandarasekhar, J.; Ramamurthy, V. *J. Chem. Soc., Chem. Commun.* **2002**, 830−831. (b) Kaanumalle, L. S.; Sivaguru, J.; Arunkumar, N.; Karthikeyan, S.; Ramamurthy, V. *J. Chem. Soc., Chem. Commun.* **2003**, 116−117. (c) Uppili, S.; Ramamurthy, V. *Org. Lett.* **2002**, *4*, 87−90.

(9) Sivaguru, J.; Shichi, T.; Ramamurthy, V. *Org. Lett.* **2002**, *4*, 4221−4224.

TABLE 1. Stereoselective Photoisomerization of *cis*-Diphenylcyclopropane Derivatives: Esters as Chiral Auxiliaries

	% diastereomeric excess (de)[a]						
medium	*trans*-**1**	*trans*-**2**	*trans*-**3**	*trans*-**4**	*trans*-**5**	*trans*-**6**	*trans*-**7**
solution[b]	4 (B)	3 (B)	5 (B)	0	4 (B)	5 (A)	4 (A)
LiY	50 (B)	25 (A)	12 (A)	14 (A)	7 (B)	2 (A)	78 (B)
NaY	55 (B)	40 (A)	32 (B)	19 (B)	16 (A)	6 (B)	19 (A)
KY	30 (B)	6 (A)	7 (A)	13 (B)	7 (A)	7 (B)	11 (A)
RbY	22 (B)	5 (A)	5 (A)	5 (B)	5 (A)	13 (B)	1 (A)
CsY	5 (B)	3 (A)	2 (A)	2 (B)	2 (A)	13 (B)	38 (B)
TlY							51 (B)
SiO_2	2 (B)	3 (A)	0	0			

[a] The first peak that elutes out of the GC/HPLC column is assigned as A and the second as B. Conversion was kept <25% (90 min irradiation). [b] A mixture of 0.5 mL of dichloromethane and 15 mL of hexane was used as solvent. 8 mL of acetonitrile as solvent gave similar results.

TABLE 2. Stereoselective Photoisomerization of *cis*-Diphenylcyclopropane Derivatives: Amide as Chiral Auxiliaries

	% diastereomeric excess (de)[a]				
medium	*trans*-**8**[c]	*trans*-**9**	*trans*-**10**	*trans*-**11**	*trans*-**12**[c,d]
solution[b]	2 (*SS*-isomer)	3 (A)	2 (B)	2 (B)	4 (*SS*-isomer)
LiY	80 (*SS*-isomer)	17 (A)	29 (B)	7 (A)	69 (*SS*-isomer)
NaY	28 (*RR*-isomer)	30 (A)	24 (A)	7 (A)	7 (*RR*-isomer)
KY	14 (*RR*-isomer)	20 (A)	26 (A)	3 (A)	33 (*RR*-isomer)
RbY	5 (*RR*-isomer)	6 (A)	29 (A)	12 (B)	0
CsY	5 (*RR*-isomer)	6 (A)	37 (A)	23 (B)	8 (*SS*-isomer)
TlY	37 (*RR*-isomer)	10 (A)			3 (*SS* isomer)
SiO_2	8 (*RR*-isomer)	7 (A)			11 (*SS* isomer)

[a] The first peak that elutes out of the GC/HPLC column is assigned as A and the second as B. Conversion was kept <25% (90 min irradiation). The absolute configurations of the isomers (except in the cases of **8** and **12**) are not known, and they are not essential to understand the mechanism of the chiral induction. [b] A mixture of 0.5 mL of dichloromethane and 15 mL of hexane was used as solvent. 8 mL of acetonitrile as solvent gave similar results. [c] The absolute configuration identified by absolute asymmetric synthesis. [d] The irradiation was done both with Pyrex and quartz cutoff. The de did not change with the mode of excitation.

(2*R*,3*R*)-1-Acetyl-2,3-diphenylcyclopropane was oxidized to (2*R*,3*R*)-diphenylcyclopropane-1-carboxylic acid (*trans*-**26**-*RR*) by the iodoform reaction (Scheme 2).[12] *trans*-**26**-*RR* was converted to *trans*-**8**-*RR*, *trans*-**12**-*RR*, and *trans*-**18**-*RR* by ETC/DMAP coupling[13] with (*S*)-(−)-1-phenylethylamine, (*S*)-(−)-1-naphthylethylamine, and L-valine methyl ester, respectively. The knowledge of the absolute configurations of **8**, **12**, and **18** is vital in understanding the role of confined medium and cations on asymmetric induction during photoisomerization.

Diastereoselective Photoisomerization of *cis*-2,3-Diphenylcyclopropane-1-carboxylic Acid Derivatives: Direct Excitation. Irradiation of *cis*-2,3-diphenylcyclopropane-1-carboxylic acid derivatives in dichloromethane/hexane (0.5 mL/15 mL) or acetonitrile (8 mL) solution gave the trans isomers with low diastereomeric excess (de) (Tables 1−4). For zeolite irradiations, following the protocol described in the Experimental Section, *cis*-2,3-diphenylcyclopropane-1-carboxylic acid derivatives were included within alkali cation (Li^+, Na^+, K^+, Rb^+, and Cs^+) exchanged Y zeolites and irradiated, and products were extracted. Mass balance was estimated by GC by using docosane as the internal standard (mass balance ∼75% for ∼30% conversion). Diastereomeric excess was calculated by either GC or HPLC analysis (<25% conversion, Tables 1−4). Lower mass balance at prolonged

TABLE 3. Stereoselective Photoisomerization of *cis*-Diphenylcyclopropane Derivatives: Amino Alcohols as Chiral Auxiliaries

	% diastereomeric excess (de)[a]		
medium	*trans*-**14**[c,d]	*trans*-**15**[c]	*trans*-**17**[e]
solution[b]	30 (A)	22 (A)	8 (A)
LiY	25 (B)	58 (A)	11 (A)
NaY	60 (A)	89 (A)	9 (A)
KY	13 (A)	15 (A)	15 (B)
RbY	2 (A)	9 (A)	23 (B)
CsY	0	5 (A)	0
TlY	3-B		

[a] The first peak that elutes out of the GC/HPLC column is assigned as A and the second as B. Conversion was kept <25% (90 min irradiation). The absolute configurations of the isomers are not known, and they are not essential to understand the mechanism of the chiral induction. [b] A mixture of 0.5 mL of dichloromethane and 15 mL of hexane was used as solvent. 8 mL of acetonitrile as solvent gave similar results. [c] The diastereomers were separated in two different columns (Chiralpak-AD-RH and Chiralpak-AD: Chiral stationary phases) on the HPLC to verify the selectivity. [d] The amide of ephedrine derivative **16** did not separate on the HPLC and did not show up in the GC; hence, the value is not reported. The ephedrine derivative **16** was attempted to observe the effect of *N*-methylation directly with respect to the norephedrine derivative **14**. [e] The diastereomeric peaks on the HPLC were very broad, and hence, the error limit might be ±5.

(10) Aggarwal, V. K.; Smith, H. W.; Hynd, G.; Jones, R. V. H.; Fieldhouse, R.; Spey, S. E. *J. Chem. Soc., Perkin Trans. 1* **2000**, 3267−3276.

(11) Aggarwal, V. K.; Thompson, A.; Jones R. V. H.; Standen, M. C. H. *J. Org. Chem.* **1996**, *61*, 8368−8369.

(12) (a) Fuson, R. C.; Bull, B. A. *Chem. Rev.* **1934**, *15*, 275. (b) Seelye, R. N.; Turney, T. A. *J. Chem. Educ.* **1959**, *36*, 572. (c) House, H. O. *Modern Synthetic Reactions*, 2nd ed.; W. A. Benjamin: Reading, MA, 1972; pp 464−465. (d) Lieben, A. *Ann. (Suppl.)* **1870**, *7*, 218. (e) March, J. *Advanced Organic Chemistry*, 4th ed.; Wiley-Interscience: New York, 1992; p 632. (f) *Vogel's Textbook of Practical Organic Chemistry*; Revised byFurniss, B. S., Hannaford, A. J., Rogers, V., Smith, P. W. G., Tatchell, A. R.; Longman Scientific & Technical, John Wiley & Sons, New York, 1978.

(13) Hassner, A.; Alexanian, V. *Tetrahedron Lett.* **1978**, *46*, 4475−4478. (b) Kress, J.; Rosner, A.; Hirsch, A. *Chem Eur J.* **2000**, *6* (2), 247−257. (c) Taha, T. S. M.; Miller, S. F. *Biochemistry* **1992**, *31*, 9090−9097.

TABLE 4. Stereoselective Photoisomerization of *cis*-Diphenylcyclopropane Derivatives: Amino Acid Derivatives as Chiral Auxiliaries

	% diastereomeric excess (de)[a]						
medium	*trans*-**18**[c]	*trans*-**19**	*trans*-**20**	*trans*-**21**	*trans*-**22**	*trans*-**23**	*trans*-**24**
solution[b]	2 (*RR*-isomer)	20 (A)	3 (A)	5 (B)	2 (A)	1 (A)	4 (B)
LiY	83 (*SS*-isomer)	39 (B)	26 (B)	34 (B)	10 (A)	21 (A)	3 (B)
NaY	21 (*RR*-isomer)	31 (A)	22 (A)	22 (A)	32 (A)	40 (A)	2 (B)
KY	80 (*RR*-isomer)	61 (A)	46 (A)	31 (A)	53 (A)	44 (A)	14 (B)
RbY	47 (*RR*-isomer)	34 (A)	22 (A)	44 (B)	32 (A)	7 (B)	4 (B)
CsY	5 (*RR*-isomer)	0	9 (A)	5 (B)	6 (A)	5 (B)	5 (B)

[a] The first peak that elutes out of the GC/HPLC column is assigned as A and the second as B. Conversion was kept <25% (90 min irradiation). [b] A mixture of 0.5 mL of dichloromethane and 15 mL of hexane was used as solvent. 8 mL of acetonitrile as solvent gave similar results. [c] The absolute configuration was identified by absolute asymmetric synthesis.

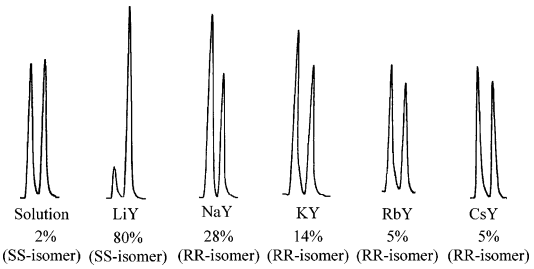

FIGURE 1. Diastereoselectivity in *trans*-**8** during photoisomerization of *cis*-**8** in various media. GC traces corresponding to *trans*-**8** are shown. Results emphasize the differences between solution and zeolites and the cation dependence.

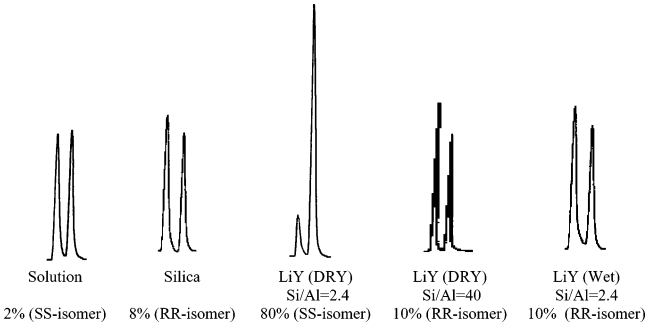

FIGURE 2. Diastereoselectivity in *trans*-**8** during photoisomerization of *cis*-**8** in various media. GC traces corresponding to *trans*-**8** are shown. Results emphasize the importance of cations during diastereoselective photoisomerization.

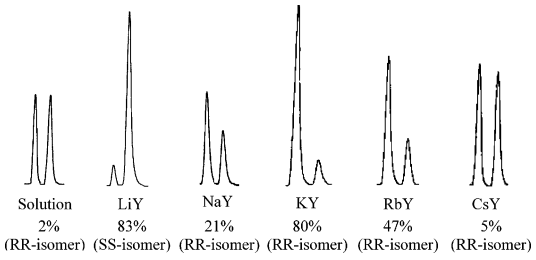

FIGURE 3. Diastereoselectivity in *trans*-**18** during photoisomerization of *cis*-**18** in various media. GC traces corresponding to *trans*-**18** are shown. Results emphasize the differences between solution and zeolites and the cation dependence.

irradiation time (>6 h) was due to the formation of side products such as indans and alkenes whose formation has previously been recorded in the literature.[14]

Perusal of Tables 1−4 reveals that the diastereoselectivities within zeolites are consistently higher than in isotropic solution. The ester derived from menthol *cis*-**1** gave 55% diastereomeric excess in NaY compared to 4% in solution. Other isomeric menthyl esters (*cis*-**2** and *cis*-**3**) gave moderate diastereoselectivity (Table 1). Based on the assumption that bulkiness of the chiral auxiliary might play a role in the chiral induction process, more bulky fenchyl ester *cis*-**5** and isopinocampheol ester *cis*-**6** and less bulky *S*-(−)-2-methyl butyl ester *cis*-**4** were examined. The diastereoselectivities observed in all of these systems within zeolites were low, even though the observed selectivity was higher than in solution. The best de was obtained with 1-phenylethyl ester *cis*-**7** (78% in LiY).

In the context of asymmetric induction a variety of amide-linked chiral auxiliaries (amides derived from amines, amino alcohols, and amino acids) were also explored. Remarkable success was observed with these systems (Tables 2−4). The very first amide examined, *S*-(−)-1-phenylethyl amide *cis*-**8**, gave 80% diastereomeric excess compared to 2% in solution. The highest chiral induction was observed with the amide derived from pseudoephedrine (*cis*-**15**; 89% in NaY). Due to additional products (formation of indans and alkenes) at longer irradiation times, the diastereoselectivity at the photostationary state could not be measured. However, the de remained the same for 90 min, 3 h, 6 h, and 12 h irradiations of *cis*-**1** and *cis*-**8**.

A number of observations suggested that alkali metal ions present in zeolites play an important role in the asymmetric induction process. (a) The de was dependent on the nature of the alkali metal ion (e.g., % de in the case of *cis*-**8** in LiY, NaY, KY, RbY, and CsY were 80, 28, 14, 5, and 5, respectively; Table 2, Figure 1). (b) The de varied with water content of NaY used (*cis*-**8**: dry, 80%, and wet, 10%; Figure 2). (c) The de upon irradiation of *cis*-**8** adsorbed on silica gel, a surface that does not contain cations, was only 8% (Figure 2). (d) Diastereomeric excess in the case of *cis*-**8** decreased from 80% to 10% when the Si/Al ratio of LiY zeolite was changed from 2.4 to 40 (Figure 2). The number of cations per unit cell decreases from 56 to 5 upon changing the Si/Al ratio from 2.4 to 40 (refer to the Experimental Section for calculation of the number of supercages and number of cations).

A closer examination of Tables 1−4 reveals that the cation not only controls the extent of diastereoselectivity but also the isomer being enhanced. The most remarkable

(14) (a) Valyocsik, E. W.; Sigal, P. *J. Org. Chem.* **1971**, *36*, 66−72. (b) Griffin, G. W.; Covell, J.; Petterson, R. C.; Dodson, R. M.; Klose, G. *J. Am. Chem. Soc.* **1965**, *87*, 1410−1411.

TABLE 5. Triplet-Sensitized Stereoselective Photoisomerization of *cis*- Diphenylcyclopropane Derivatives

	% diastereomeric excess (de)[e]					
medium[a]	*trans*-**7**	*trans*-**8**[d]	*trans*-**9**	*trans*-**14**	*trans*-**18**[d]	*trans*-**24**
solution[b]	16 (A)	15 (*RR*-isomer)	17 (A)	7 (A)	0	7 (B)
LiY	75 (B)	33 (*SS*-isomer)	52 (A)	23 (B)	52 (*SS*-isomer)	3 (B)
NaY	46 (B)	40 (*RR*-isomer)	61 (A)	59 (B)	18 (*RR*-isomer)	8 (B)
KY	18 (B)	61 (*RR*-isomer)	8 (A)	43 (B)	81 (*RR*-isomer)	17 (B)
RbY	44 (B)	15 (*RR*-isomer)	2 (A)	17 (B)	45 (*RR*-isomer)	4 (B)
CsY	72 (B)	2 (*RR*-isomer)	7 (A)	1 (B)	13 (*RR*-isomer)	0
TlY[c]	51 (B)	37 (*RR*-isomer)	10 (A)	3 (B)		

[a] *p*-Methoxyacetophenone used as the sensitizer for all zeolite irradiation. Loading level of the sensitizer kept at one molecule per supercage; substrate: one molecule per 12 supercages for all zeolite irradiation (24 h irradiation). [b] Acetone was used as the sensitizer and solvent (90 min irradiation). Sensitization with *p*-methoxyacetophenone as sensitizer in solution (CH_2Cl_2/hexane) gave similar results. [c] Direct irradiation (90 min irradiation). No sensitizer was employed. [d] The absolute configuration of isomers was determined by absolute asymmetric synthesis. [e] The first of the two diastereomeric peaks was assigned as A and the second peak as B.

example is provided by the amide derived from L-valine methyl ester *cis*-**18**. Within LiY the *trans*-**18**-*SS* was favored to 83% in excess, whereas in KY *trans*-**18**-*RR* was favored to 80% in excess (Scheme 1, Figure 3, Table 4). A similar alkali ion dependent diastereomer switch was observed in the case of *cis*-**8**; LiY favored *trans*-**8**-*SS* to 80% excess, and NaY favored *trans*-**8**-*RR* to 28% excess. Enhancement of one isomer in LiY and the other diastereomer in NaY−CsY was true with many diphenylcyclopropane systems (Tables 1−4).[6a] To confirm that the cation-dependent diastereomer switch was not due to an overlapping impurity, the diastereoselectivities in selected cases were monitored both by GC and HPLC.[15] Both analyses gave the same results.

While investigating a series of amides derived from chiral amino alcohols (Table 3), we noticed that the cation-dependent diastereomer switch was absent in the case of the amide derived from (−)-pseudoephedrine *cis*-**15** while it was observed in the case of the amide derived from (−)-norephedrine *cis*-**14**. The only difference between the chiral auxiliary employed in the above two cases is that N−H in (−)-norephedrine is replaced with N−CH_3 in (−)-pseudoephedrine. If indeed *N*-methylation prevents the cation-dependent diastereomer switch as observed in the case of (−)-pseudoephedrine, then it should be effective in other chiral auxiliaries with an N−H group. The two N−H amides that showed the cation-dependent diastereomer switch with high stereoselectivity *cis*-**8** and *cis*-**18** were *N*-methylated to the corresponding *N*-methyl derivatives *cis*-**9** and *cis*-**24**, respectively. The photoisomerization of *N*-methyl-1-phenylethyl amide derivative *cis*-**9** and *N*-methyl-L-valine methyl ester derivative *cis*-**24** was studied within alkali metal ion (Li^+, Na^+, K^+, Rb^+, and Cs^+) exchanged Y-zeolite. In both cases, cation-dependent diastereomer switch was not observed (Tables 2 and 4).

Diastereoselective Photoisomerization of *cis*-2,3-Diphenylcyclopropane-1-carboxylic Acid Derivatives: Triplet Sensitization. Acetone and *p*-methoxyacetophenone sensitization of *cis*-diphenylcyclopropane derivatives **7**, **8**, **9**, **14**, **18**, and **24** in solution gave the corresponding *trans*-isomers with de varying between 0 and 17% (Table 5). Although direct excitation resulted in side products (alkene and indan), triplet sensitization both in solution as well as within zeolites gave mainly the products of geometric isomerization, and the photostationary state was achieved within 24 h in zeolites. Photoisomerization was efficient when the triplet energy of the sensitizer (E_T) was higher than 69 kcal/mol (e.g., acetone and acetophenone) and inefficient with sensitizers having triplet energy lower than 69 kcal/mol, viz. fluorenone (E_T = 50.9 kcal/mol), benzil (E_T = 53 kcal/mol), acetonaphthone (E_T = 59.9 kcal/mol), and benzophenone (E_T = 67 kcal/mol).[16]

Photoisomerization by triplet sensitization was performed by including the sensitizer (acetophenone derivatives) and *cis*-2,3-diphenylcyclopropane-1-carboxylic acid derivatives (Scheme 1) within alkali ion (Li^+, Na^+, K^+, Rb^+, Cs^+, and Tl^+) exchanged Y zeolites. The experimental procedures adopted for inclusion of reactants within zeolites, irradiation, and extraction and analysis of products are described in the Experimental Section.

TABLE 6. Asymmetric Photoisomerization of *cis*-8 with Various Loading Levels of the Sensitizer Inside KY Zeolite

loading level of the sensitizer[a]	*cis*-**8** : *trans*-**8** after irradiation	% de (*trans*-**8**)[b]
9.9	78:22	54 (*RR*-isomer)
3.96	75:25	48 (*RR*-isomer)
1.98	65:35	55 (*RR*-isomer)
1.32	57:43	54 (*RR*-isomer)
1.00	45:55	63 (*RR*-isomer)
0.79	49:51	56 (*RR*-isomer)

[a] *p*-Methoxyacetophenone (4MAP) was used as the sensitizer for all zeolite irradiation. The reaction was performed inside dry KY zeolite, 24 h irradiation with positive N_2 pressure. Loading level is defined as the number of supercages per molecule of the sensitizer. For calculation of the number of supercages refer to the Experimental Section. [b] The absolute configuration of the isomer was determined by absolute asymmetric synthesis.

TABLE 7. Triplet-Sensitized Photoisomerization of *cis*-8 and *cis*-18 with Various Sensitizers

	% diastereoselectivity[a−c]	
sensitizer	*trans*-**8**	*trans*-**18**
acetophenone	75 (*RR*-isomer)	85 (*RR*-isomer)
p-methoxyacetophenone	61 (*RR*-isomer)	81 (*RR*-isomer)
p-cyanoacetophenone[d]	57 (*RR*-isomer)	43 (*RR*-isomer)
p-methylacetophenone	50 (*RR*-isomer)	78 (*RR*-isomer)
p-fluoroacetophenone	45 (*RR*-isomer)	36 (*RR*-isomer)
p-chloroacetophenone	40 (*RR*-isomer)	71 (*RR*-isomer)
xanthone	30 (*RR*-isomer)	40 (*RR*-isomer)

(15) Refer to the Supporting Information for details.

(16) (a) Hixson, S. S.; Boyer, J.; Gallucci, C. *J. Chem. Soc., Chem. Commun.* **1974**, 540−542. (b) Sivaguru, J.; Jockusch, S.; Turro, N. J.; Ramamurthy, V. *Photochem. Photobiol. Sci.* **2003**, *2(11)*, 1101−1106.

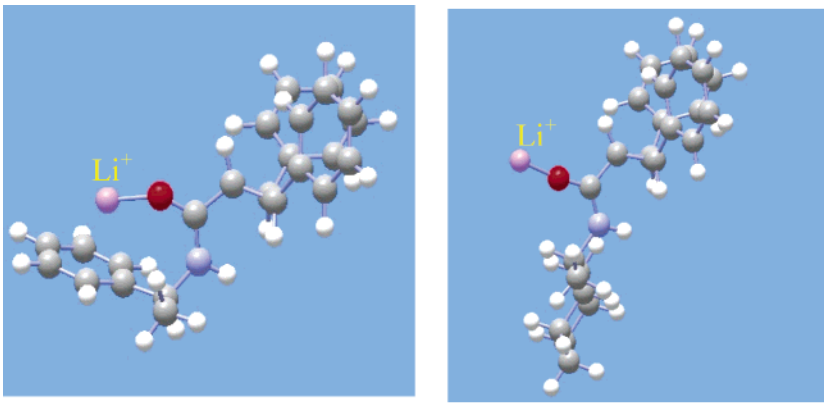

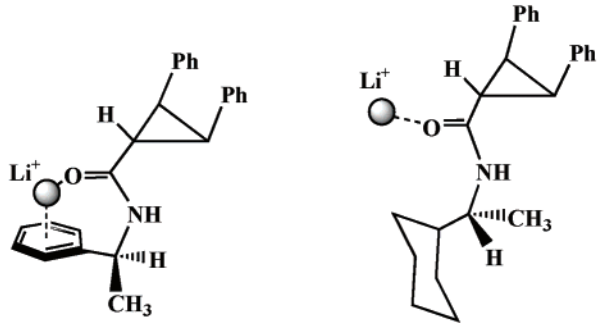

cis-**8** *cis*-**10**

Compound	Binding Affinity (kcal/mol)	C=O---M^+ distance (Å)	Benzene---M^+ distance (Å)	C=O---M^+ Angle (degrees)
cis-**8**	91.3	1.73	2.09	140.4°
cis-**10**	80.26	1.65	-	171.4°

FIGURE 4. Binding affinities and structural details of Li^+-bound *cis*-**8** and *cis*-**10** optimized at the RHF/3-21G level.

Results of product studies are summarized in Table 5. The extent of diastereoselectivity as shown in Table 6 was independent of the loading level of the triplet sensitizer (e.g., *cis*-**8**). This observation supports the view that the photoisomerization occurs only from the triplet state and is triggered by the sensitizers. Had there been photoisomerization that is not triggered by the sensitizer, the selectivity would have been different with different loading levels of the sensitizer (Table 6).

The importance of cations in the diastereoselective process is evident from the following observations: The diastereoselectivity during photoisomerization of *cis*-**8** within wet KY zeolite (intentionally exposed to water) was only 14%, whereas within dry KY it was 61%. Sensitized photoisomerization of *cis*-**8** adsorbed on silica surface, a medium that lacks cation, gave low de (12%). Direct irradiation of TlY zeolite gave product distribution similar to triplet-sensitized irradiation, which is most likely due to the heavy cation effect (Tl^+)-induced intersystem crossing from the singlet to triplet state.[5a]

As mentioned above, efficient photoisomerization was observed when the triplet energy of the sensitizer (E_T) was higher than 69 kcal/mol. However, for substituted acetophenone sensitizers with similar triplet energies the substituent on the aryl ring determined the extent of diastereoselectivity. While all sensitizers listed in Table 7 efficiently isomerized *cis*-**8** and *cis*-**18**, the observed diastereoselectivities in the products within KY were not the same. We believe that the site of cation binding to the sensitizer plays a role in this process. It is quite likely that the substituent on the aryl ring alters the manner in which the cation is bound to the sensitizer and the reactant. Further studies are needed to understand this phenomenon.

The following observations concerning diastereoselective photoisomerization in the triplet state are noteworthy: (a) The diastereomeric excesses obtained under sensitized conditions are different from the ones obtained upon direct excitation. (b) The diastereoselectivity was dependent on the nature of the cation within the zeolite; high selectivity was usually observed within NaY or KY. (c) Although the phenomenon of cation-dependent diastereomer switch is observed also during triplet sensitization, the results are not identical to the ones obtained during direct excitation. For example, in the case of *cis*-**7** and *cis*-**14** the switch is observed under direct excitation but not under triplet sensitization. In the case of *cis*-**8** and *cis*-**18**, although the switch is

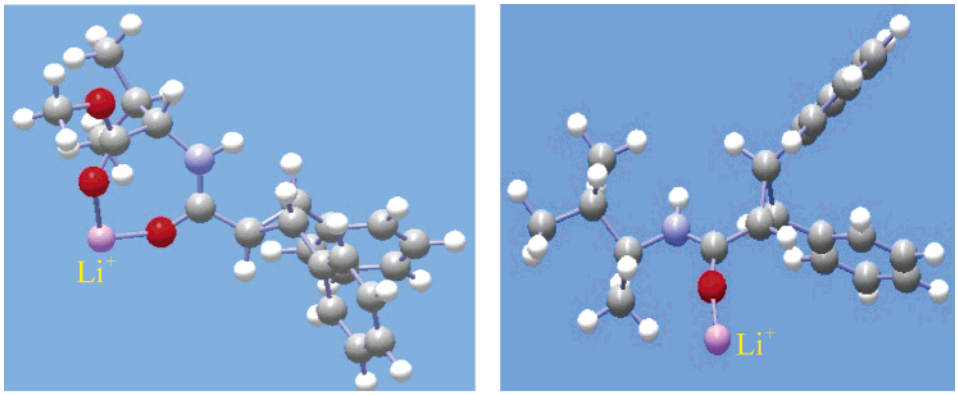

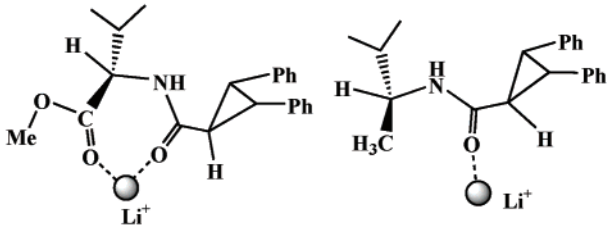

cis-**18** *cis*-**11**

Compound bound to Li^+	Binding Affinity (kcal/mol)	(ester)C=O---Li^+ distance (Å)	(Amide)C=O---Li^+ distance (Å)	Angle (degrees)
cis-**18**----Li^+	104.10	1.78	1.76	O---Li---O 103.8°
cis-**11**----Li^+	80.26	-	1.65	C=O---Li 171.0°

FIGURE 5. Binding affinities and structural details of Li^+-bound *cis*-**11** and *cis*-**18** optimized at the RHF/3-21G level.

observed, the extent of de in various zeolites under both conditions is not the same. (d) The observed diastereoselectivity was independent of the duration of irradiation (e.g., % de in *trans*-**8**: 12 h, 57%; 24 h, 60%; 48 h, 61% and 72 h, 61%).

Recognizing the importance of cations in asymmetric induction process, the photoisomerization of *cis*-**8** and *cis*-**18** were carried out in the presence of 1 M $LiClO_4$ and $NaClO_4$ in acetone that served both as a solvent and sensitizer. The diastereoselectivity remained the same in the presence and absence of alkali ion salts. Probably, the factors that make the perchlorate salt soluble in acetone, solvation of the cation by the solvent, makes the cation inaccessible to the reactant molecule. In the case of a zeolite, which provides a medium of "naked cations" ensures an interaction between the reactant molecule and the cation.

Discussion

Results presented in Tables 1−5 establish that a chiral auxiliary functions better within a zeolite than in an organic solvent both during direct excitation and triplet sensitization. Further, the cations present within a zeolite appear to play an important role in the chiral induction process. It has been established that direct excitation results in isomerization from S_1 (with no triplet contribution) and triplet sensitization leads to reaction from T_1.[16−18]

Although with the results on hand we cannot provide a detailed understanding of the process, we believe that we are in a position to point out some of the important factors that control the diastereoselectivity within zeolites. Examination of Tables 1−4 (24 chiral auxiliaries employed) reveals that aryl chiral auxiliaries (e.g., **7**, **8**, **12**, **14**, and **15**) are more effective than alkyl chiral auxiliaries (e.g., **10**) within zeolites.[6a,8a,b] For example, *cis*-2,3-diphenylcyclopropane-1-carboxamides with phenyl chiral auxiliary *cis*-**8**, the naphthyl chiral auxiliary *cis*-**12**, and systems based on amino alcohol chiral auxiliaries *cis*-**14** and *cis*-**15** gave 80% (LiY), 69% (LiY), 60% (NaY), and 89% (NaY) de. However, the *cis*-2,3-diphenylcyclopropane-1-carboxamide appended with alkyl chiral auxiliary (cyclohexyl as in *cis*-**10** instead of phenyl as in *cis*-**8**) gave only 29% de. Several chiral esters containing

(17) Griffin, G. W.; Covell, J.; Petterson, R. C.; Dodson, R. M.; Klose, G. *J. Am. Chem. Soc.* **1965**, *87*, 1410−1411.

(18) (a) Hixson, S. S. In *Organic Photochemistry*; Padwa, A., Ed.; Marcell Dekker: New York, 1979; Vol. 4, pp 191−260 and selected references therein. (b) Hixson, S. S.; Garrett, D. W. *J. Am. Chem. Soc.* **1974**, *96*, 4872−4879. (c) Hixson, S. S. *J. Am. Chem. Soc.* **1974**, *96*, 4866−4871.

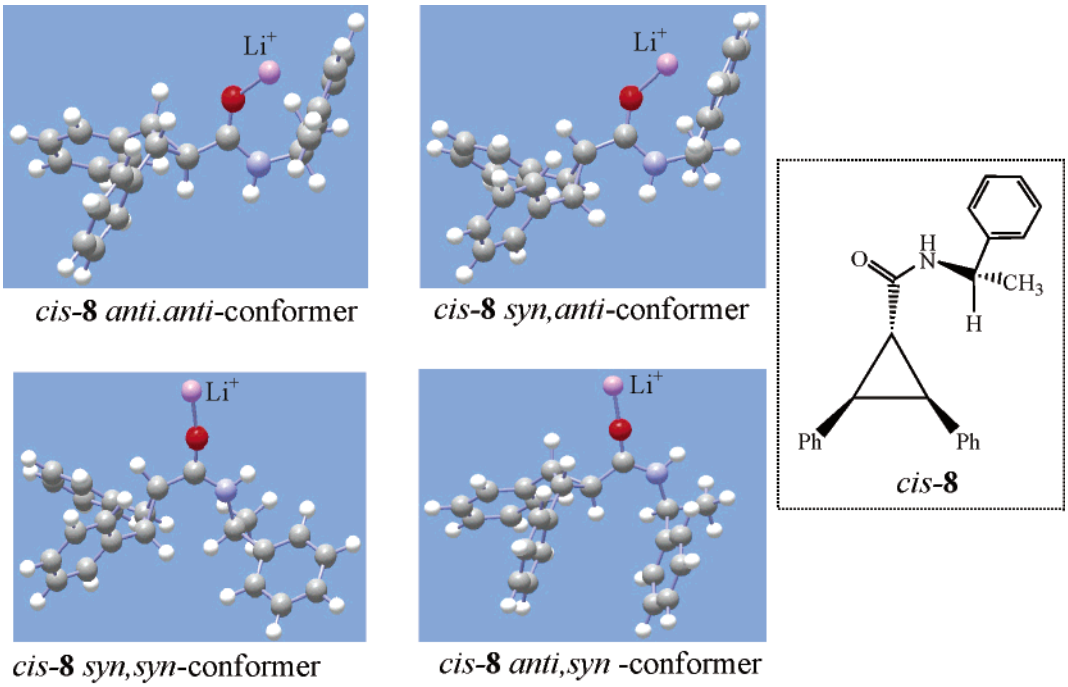

Geometry	B.A. (kcal/mol)	C=O---M^+ Distance (Å)	Benzene[a]--M^+ Distance (Å)	C---O---M^+ Angle
anti,anti-conformer	79.19	1.80	2.01	134.86°
syn,anti-conformer	80.51	1.80	2.01	136.43°
anti,syn-conformer	64.39	1.70	-	175.80°
syn,syn-conformer	68.64	1.71	-	168.99°

a) The benzene ring of the chiral auxiliary.

FIGURE 6. Binding affinities and structural details of Li^+ bound to various conformers of *cis*-**8** optimized at RB3LYP/6-31G*.

alkyl substituents (e.g., *cis*-**2**, -**3**, -**4**, -**5**, and -**6**: <25% in LiY) gave lower de than the phenyl ester *cis*-**7** (de, 78% in LiY). Although we did not examine the triplet-sensitized photochemistry of several systems we are confident that the above trend will be maintained during triplet-sensitized isomerization as well. In our laboratory, we have observed similar trend with several other photoreactions as well.[6a]

An insight into how cations play a role in the above chiral discrimination process is revealed by the results of ab initio computations of several 2,3-diphenylcyclopropane-1-carboxamides. While one may question the value of gas-phase computational data in understanding the chemical behavior of molecules within a zeolite, a much more complex environment, we find them useful as a guide in building a preliminary model. The binding affinities and geometries (Figure 4) of Li^+ bound *cis*-**8** (representing aryl chiral auxiliary) and *cis*-**10** (representing alkyl chiral auxiliary) computed at the restricted Hartree−Fock level (RHF/3-21G) level[19] provided insight into the role of aryl group in enhancing the power of a chiral auxiliary within zeolites. Both molecules interacted strongly with Li^+ with binding affinities >80 kcal/mol. Since alkali metal ions are bound to the surface of a zeolite, the binding affinities between the cation and the guest molecules within a zeolite are expected to be smaller than the values computed above, but the trend is likely to remain the same. In the case of *cis*-**8** (with aryl chiral auxiliary), the cation interacts simultaneously with phenyl group by cation−π interaction[20] as well as with the amide carbonyl oxygen by dipolar interaction[21,22] (Figure 4, left side). Such interactions are expected to reduce the rotational freedom of the chiral auxiliary and thus make it "rigid". On the other hand, in the case of *cis*-**10** (with alkyl chiral auxiliary) the cation interacts only with the amide carbonyl oxygen via dipolar-type interaction (Figure 4, right side). Such an interaction would have no effect on the rotational mobility of the chiral auxiliary. A model based on cation-binding-dependent flexibility of the chiral auxiliary accounts for the observed variation in de between aryl and alkyl chiral auxiliaries within zeolites.

(19) *Gaussian 98, Revision A.9;* Gaussian, Inc.: Pittsburgh, PA, 1998.

(20) Ma, J. C.; Dougherty, D. A. *Chem. Rev.* **1997**, *97*, 1303−1324.

(21) Raber, D. J.; Raber, N. K.; Chandrasekhar, J.; Schleyer, P. v. R. *Inorg. Chem.* **1984**, *23*, 4076.

(22) (a) Dunbar, R. C. *J. Phys. Chem. A* **2000**, *104*, 8067−8074. (b) Siu, F. M.; Ma, N. L.; Tsang, C. W. *J. Am. Chem. Soc.* **2001**, *123*, 3397−3398. (c) Jockusch, R. A.; Lemoff, A. S.; Williams, E. R. *J. Am. Chem. Soc.* **2001**, *123*, 12255−12265. (d) Wyttenbach, T.; Witt, M.; Bowers, M. T. *J. Am. Chem. Soc.* **2000**, *122*, 3458−3464. (e) Jockusch, R. A.; Price, W. D.; Williams, E. R. *J. Phys. Chem. A* **1999**, *103*, 9266−9274. (f) Hoyau, S.; Ohanessian, G. *Chem. Eur. J.* **1998**, *4*, 1561−1569.

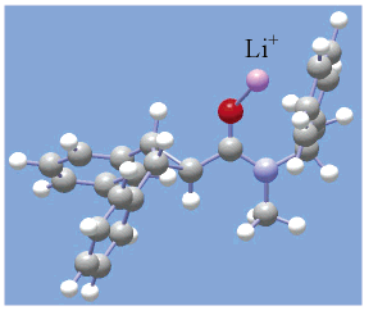

cis-**9** *anti,anti*-conformer

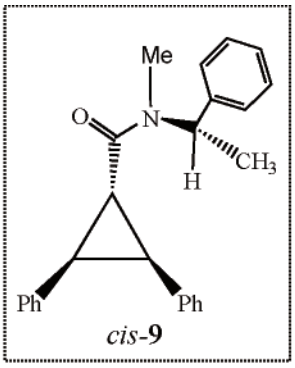

cis-**9**

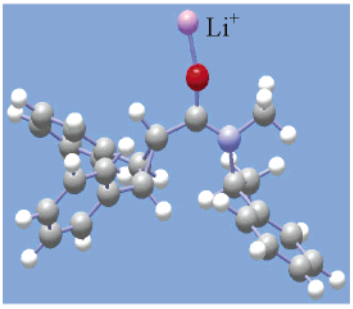

cis-**9** *syn,syn*-conformer

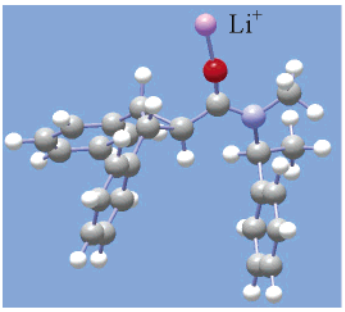

cis-**9** *anti,syn*-conformer

Geometry	B.A. (kcal/mol)	C=O---M^+ Distance (Å)	Benzene[a]---M^+ Distance (Å)	C---O---M^+ Angle
anti,anti-conformer	79.76	1.79	2.00	136.86°
syn,anti-conformer[a]	79.76	1.79	2.00	136.86°
anti,syn-conformer	64.76	1.70	-	171.66°
syn,syn-conformer	68.52	1.70	-	165.29°

a) *syn,anti*-conformer **9** optimization resulted in *anti,anti*-conformer **9** and hence the binding affinity is the same.

FIGURE 7. Binding affinities and structural details of Li^+ bound to various conformers of *cis*-**9** optimized at RB3LYP/6-31G*.

The above model works well also in the case of amino acid derived chiral auxiliaries. The structures *cis*-**11** and *cis*-**18** differ only with respect to the substituent on the chiral auxiliary; the methyl group in *cis*-**11** is replaced by a carbomethoxy group in *cis*-**18**. This change in structure has a significant impact on the observed de within LiY (*cis*-**18**, 83%; *cis*-**11**, 7%). Both *cis*-**11** and *cis*-**18** interacted strongly with Li^+ (Figure 5) with binding affinities >80 kcal/mol. In the case of *cis*-**18** (with carbomethoxy chiral auxiliary), Li^+ interacts simultaneously with both the carbonyl of the carbomethoxy group and the amide carbonyl oxygen. Such an interaction is expected to reduce the rotational freedom of the chiral auxiliary and thus make it "rigid" as in the case of the aryl chiral auxiliary. On the other hand, in the case of *cis*-**11** the cation interacts only with the amide carbonyl oxygen via a dipolar-type interaction (as in the case of *cis*-**10**). Such a type of interaction would have no effect on the rotational mobility of the chiral auxiliary. In general, amino acid derived chiral auxiliaries gave higher diastereoselectivities within zeolites compared to that in solution (Table 4).

Recently, Nau et al.,[23] based on intramolecular energy transfer measurements, provided a measure of the flexibility of the amino acids as: Gly > Ser > Asp, Asn, Ala > Thr, Leu > Phe, Glu, Gln > His, Arg > Lys > Val > Ile > Pro. It is encouraging to note that the observed diastereoselectivites within the KY zeolite upon direct irradiation of diphenylcyclopropane derivatives with amino acid derivatives as chiral auxiliaries also follow the same trend: Ala = 31%; Leu = 46%; Phe = 53%; Val = 80% (Table 4). We believe that rigidity of the chiral auxiliary is very crucial in determining the extent of diastereoselectivity. The lower the flexibility (more rigid the chiral auxiliary), the higher the selectivity. The above model applies for both direct and triplet-sensitized isomerizations.

Examination of Tables 1−4 clearly indicates that the cation not only controls the extent of diastereoselectivity but also the isomer being enhanced. For the sake of brevity, we restrict the discussion to amide derivatives. The diastereomer switch occurs both during direct excitation and triplet sensitization of *cis*-**8** and *cis*-**18**, although in the case of *cis*-**14** this occurs only during direct excitation. The most remarkable example is pro-

(23) Huang, F.; Nau, W. M. *Angew Chem., Int. Ed.* **2003**, *42*, 2269−2272.

SCHEME 3

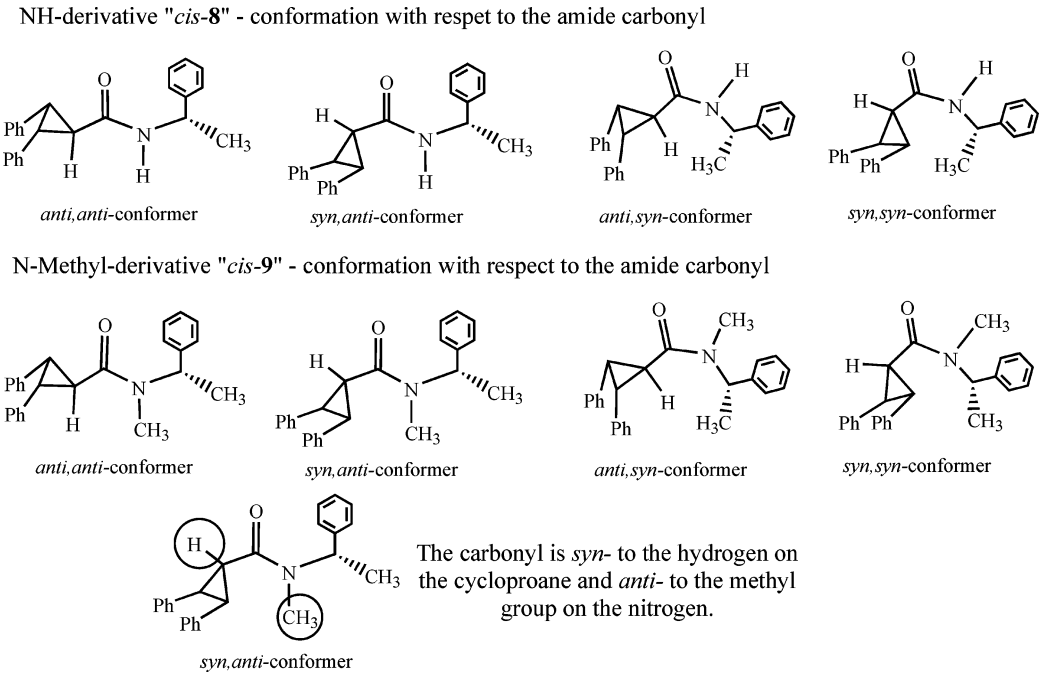

vided by the amide derived from L-valine methyl ester *cis*-**18** (Figure 3). Within LiY, the *trans*-**18**-*SS*-isomer was favored to 83% in excess, whereas in KY, the *trans*-**18**-*RR*-isomer was favored to 80% in excess. In the case of *cis*-**8** (Figure 1), LiY favored *trans*-**8**-*SS* (80% excess) and NaY favored *trans*-**8**-*RR* (28% excess). Similar striking results were also observed during triplet sensitization of *cis*-**8** and *cis*-**18** (Table 5). Triplet sensitization of *cis*-**18** within LiY *trans*-**18**-*SS* was favored (de 52%), whereas in KY *trans*-**18**-*RR* was favored (de 81%). In the case of *cis*-**8**, LiY favored formation of *trans*-**8**-*SS* (de 33%) and KY favored *trans*-**8**-*RR* (de 61%). One possibility is that different cations bind to different sites on the reactant molecule leading to cation-dependent diastereomer switch. This suggestion, although in our case has no experimental support, has literature precedence.[24c−f] On the basis of density functional calculations and low energy collisionally activated and thermal radiative dissociation experiments, a difference in binding pattern between Li^+ and K^+ ions with valine[22c] and glycine[22d,f] has been proposed. For example, Li^+ binds to these molecules through N, O coordination (oxygen on the carboxyl group and nitrogen on the amino group), whereas K^+ binds through O, O coordination (oxygens on the carboxyl moiety). A similar switch in the binding site has also been reported during the interaction of Li^+ and Cs^+ to arginine.[22e] Such a phenomenon could be involved within a zeolite and responsible for the observed cation-controlled diastereomer switch within a zeolite.

An examination of Tables 1−4 reveals that the above diastereomer switch during both direct excitation and triplet sensitization depends on whether the amide nitrogen is substituted with a hydrogen atom or methyl group. While NH derivatives showed diastereomer switch, the corresponding $N-CH_3$ derivatives did not (compare *cis*-**14** with *cis*-**15**; *cis*-**8** with *cis*-**9**, and *cis*-**18** with *cis*-**24**; Tables 2−4). As illustrated in Scheme 3, the amides being investigated, based on the rotation around cyclopropyl−carbonyl and carbonyl−N of the amide linkage, could adopt four conformations. For simplicity we have used the nomenclatures used in Scheme 3 to identify the four conformers.

Restricted rotation around the carbonyl−N bond in amides is well documented in the literature.[24] For example, in the case of *N*-methylformamide the energy for rotation (E_{rot}) was calculated to be around 0.4 kcal/mol and in the case of *N*,*N*-dimethylformamide the energy for rotation (E_{rot}) was estimated to be around ∼3.82 kcal/mol.[24] Based on this, one would expect the rotational barrier for interconversion between syn and anti conformations (with respect to the carbonyl−N bond) in *cis*-**8** to be much smaller than in *cis*-**9**.

^1H NMR and $^1H-^1H$ COSY spectra suggest that *cis*-**9** exists as two distinct conformers while *cis*-**8** exists as a single averaged conformer in solution. Two doublets for α-methyl benzyl protons and two quartets for the benzylic hydrogen of the chiral auxiliary corresponding to two conformers are seen in the ^1H NMR spectra of *cis*-**9**. This suggests that the two conformers of *cis*-**9** are thermodynamically stable and do not interconvert at room temperature in solution. Also, ^1H NMR spectra reveal that the two conformers are not present in equal amounts in solution at room temperature. On the other hand, in the case of *cis*-**8** only one doublet for α-methyl and a single quintet for benzylic hydrogens are recorded in the ^1H NMR, suggesting that the two conformers are in fast equilibrium in solution. The NMR results suggest, as expected, a higher barrier for rotation around the amide bond ($OC-NCH_3$) in *cis*-**9** than (OC−NH) in *cis*-**8**. We believe that rotation around the cyclopropyl−carbonyl

(24) (a) Wiberg, K. B.; Rush, D. J. *J. Org. Chem.* **2002**, *67*, 826−830. (b) Wiberg, K. B.; Rush, D. J. *J. Am. Chem. Soc.* **2001**, *123*, 2038−2046. (c) Wiberg, K. B.; Rablen, P. R.; Rush, D. J.; Keith, T. A. *J. Am. Chem. Soc.* **1995**, *117*, 4261−4270. (d) LeMaster, C. B.; True, N. S. *J. Phys. Chem.* **1989**, *93*, 1307−1311. (e) Ross, B. D.; True, N. S. *J. Am. Chem. Soc.* **1984**, *106*, 2451−2452. (f) Alemán, C. *J. Phys. Chem. A* **2002**, *106*, 1441−1449.

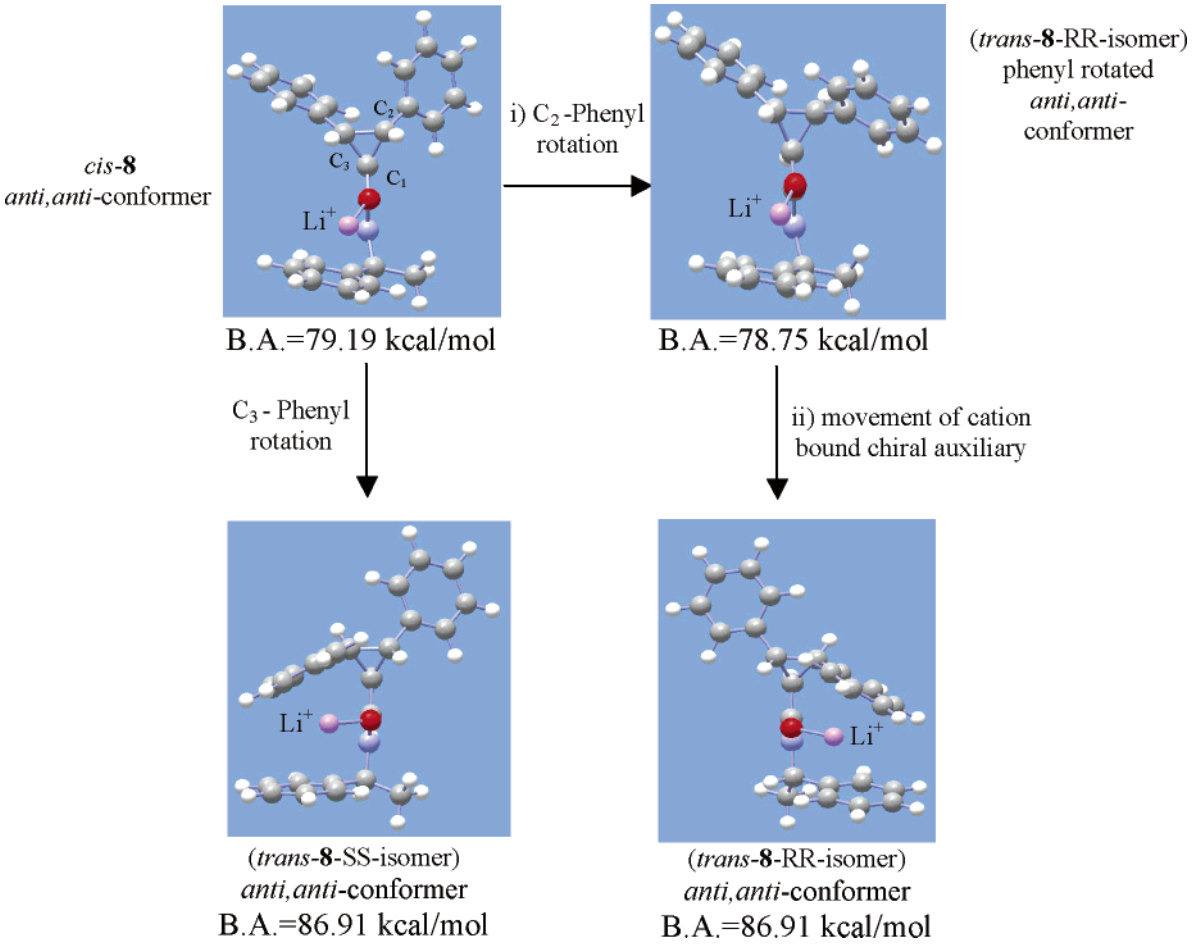

FIGURE 8. Photoisomeriztion of Li^+-bound *cis*-**8** *anit,anti*-conformer through rotation of C_2-phenyl and C_3-phenyl. Binding affinities and structural details optimized at RB3LYP/6-31G*. As per this model, isomerization via C_3-phenyl rotation would be preferred.

bond most likely has a small barrier and syn and anti conformations around this bond equilibrate fairly rapidly in both N−H and N−CH_3 systems in solution. We visualized that within a zeolite depending on the cation one of the four conformers of *cis*-**8** would be preferred leading to cation dependent diastereomer switch. In other words, one thought was that the cation-dependent diastereomer switch has its origin on the cation-dependent conformer preference within a zeolite.

To gain a better insight on the role of cation binding to different conformers of *cis*-**8** and *cis*-**9** and its effect on the observed cation-dependent diastereomer switch, density functional theory and ab initio calculations were performed at the RB3LYP/6-31G* level.[19] Binding affinities for Li^+-bound structures for *cis*-**8** and *cis*-**9** (RB3LYP/6-31G* level) are given in Figures 6 and 7. In the case of Li^+-bound *cis*-**8**, of the four conformers examined (*anti,anti*-, *syn,anti*-, *anti,syn*-, and *syn,syn*; Figure 6), the first two were more stable than the latter two; the Li^+-bound *anti,anti*- and *syn,anti*-conformers have almost the same energy (Figure 6). On the other hand, in the case of *cis*-**9** cation binding leads to only one most stable conformer, i.e., *anti,anti*- (Figure 7). During geometry optimization, to our surprise, the Li^+-bound *syn,anti*-conformer of *cis*-**9** transformed itself to the Li^+-bound *anti,anti*-conformer (Figure 7). This is most likely due to steric interaction between the N−CH_3 and cyclopropyl C−H hydrogens in the cation-bound *syn,anti*- conformation. If this trend is maintained within a zeolite, cation-bound *cis*-**9**, irrespective of the cation, will adopt only the *anti,anti*-conformation. This could translate into the cation-independent diastereomer enhancement. In the case of *cis*-**8**, according to NMR, all four conformers (*anti,anti*-, *syn,anti*-, *anti,syn*-, and *syn,syn*-) having nearly the same energies equilibrate in solution. According to calculated data, upon Li^+ binding *anti,anti*- and *syn,anti*-conformers are distinctly more stable than *anti,syn*- and *syn,syn*-conformers. Thus, within a zeolite only these two conformers are expected to be present. It is quite possible that within a zeolite depending on the alkali ion one of the two conformers is preferred, leading to cation-dependent diastereomer switch. Interestingly, computational results discussed below suggest that Li^+-bound *anti,anti*- and *syn,anti*-conformers of *cis*-**8** would give different amounts of *trans*-**8**-*RR* and *trans*-**8**-*SS*. This provides a hope that the model based on cation controlled conformational preference may have some validity. Unfortunately, at this stage we are unable to provide any experimental support for this suggestion.

As shown in Figures 8 and 9, the *trans*-**8**-*SS* is expected to be formed from *cis*-**8** via phenyl rotation at the C_3 carbon and *trans*-**8**-*RR* via phenyl rotation at the C_2 carbon. The question is whether both *anti,anti*- and *syn,anti*-conformers of *cis*-**8** would give the same amounts

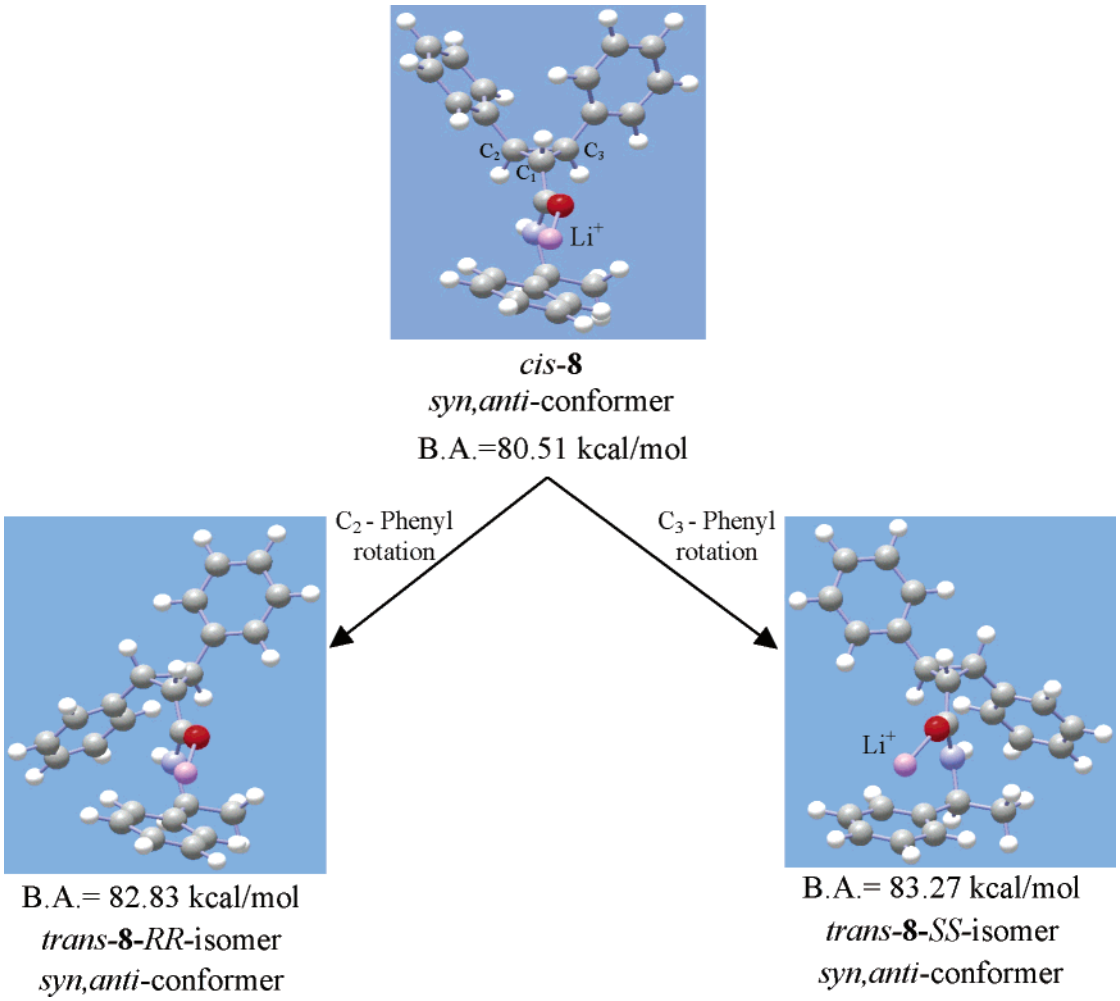

FIGURE 9. Photoisomeriztion of Li^+-bound *cis*-**8** *syn,anti*-conformer through rotation of C_2-phenyl and C_3-phenyl. Binding affinities and structural details optimized at RB3LYP/6-31G*. As per this model, isomerization via both C_3-phenyl and C_2-phenyl rotation would be equally preferred.

of *trans*-**8**-*RR* and *trans*-**8**-*SS*. In the absence of cations, both rotations are equally possible, and therefore, diastereoselectivity is expected to be small. However, Li^+ binding to the two conformers makes a difference. As seen in Figure 8, *trans*-**8**-*SS* is more easily formed from the Li^+-bound *anti,anti*-conformer of *cis*-**8**. Rotation around the C_3 carbon is helped by the developing cation$-\pi$ interaction[20] with the C_3-phenyl. Rotation around the C_2-carbon does not result in any such stabilization. Based on this, one would predict that the *trans*-**8**-*SS* isomer would be formed in excess upon excitation of Li^+ bound *anti,anti*-conformer of *cis*-**8**. On the other hand, as seen in Figure 9, computational results suggest that *trans*-**8**-*SS* and *trans*-**8**-*RR* isomers would be formed in near equal amounts from *syn,anti*-conformer of *cis*-**8**. As illustrated in Figure 9 rotation of C_2-phenyl or C_3-phenyl does not result in any significant extra stabilization by Li^+ ion. Thus it is clear that Li^+-bound *anti,anti*- and *syn,anti*-conformers of *cis*-**8** would not give *trans*-**8** with the same de. How much de is obtained and which isomer is obtained in excess will depend on which one of the two conformers is preferred within a zeolite. One wonders whether selective formation of *trans*-**8**-*SS* within LiY is an indication of *anti,anti*-conformer being preferred when *cis*-**8** is included within the zeolite. We do not have an experimental verification of this prediction. Undoubtedly, there are problems in the above approach. Computations refer to ground-state structures while reactions originate from excited singlet and triplet states. Computations deal with closed shell molecules while the reaction involve diradical and zwitterionic intermediates. Despite these deficiencies, we are pleased to note that the ab initio computational data of the ground-state structures of Li^+–*cis*-**8** complexes provided an insight into the cause of diastereoselectivty within alkali ion exchanged Y zeolites. The fact that different amounts of diastereoselectivities were obtained for the same systems during direct excitation and triplet sensitization suggests that nature of excited state and the intermediates involved should be taken into consideration while predicting asymmetric induction within zeolites. We are attempting to make progress in this direction.

Conclusion

The zeolite interior is clearly able to enhance the power of a chiral auxiliary during reaction from excited singlet and triplet states. In doing so, both the confined space as well as the cations present in a zeolite are used effectively by the zeolite. The cations and confined space

coerce the molecule to adopt a conformation resulting in a stronger interaction between the chiral center and the site of reaction present within a single molecule. The very low diastereomeric excess in most cases in solution suggests that the conformation of the reactant molecule is likely to be such that the chiral auxiliary and the reactive site of the molecule are far apart. Within the confined space of a zeolite, the cations force the molecule to adopt a folded conformation there by bringing chiral environment closer to the reactant part. Interactions between chiral auxiliary, cation and the reaction site play an important role in the overall asymmetric induction process within a zeolite. The cations not only control the extent of selectivity but also the stereoisomer being enhanced in the photoreaction. Potential of the phenomenon presented in this report in photochemical and thermal reactions is limitless. One wonders whether the zeolite scaffold does play any role other than presenting a "naked" cation to the reactants to interact with. We are exploring the effect of cations in solution to bring about the selectivity observed inside zeolite.

Experimental Section

NaY zeolite was obtained from Zeolyst International, The Netherlands. Monovalent cation-exchanged zeolites (LiY, KY, RbY, and CsY) were prepared by refluxing 10 g of NaY with 100 mL of a 10% solution of the corresponding metal nitrate in water for 24 h. The exchanged zeolite was filtered and washed thoroughly with distilled water. This procedure was repeated three times. Subsequently, the cation-exchanged zeolite was dried at 120 °C for about 3 h and stored.

All solvents were used as purchased. THF was dried over sodium/benzophenone under nitrogen prior to use. Deionized water was used when needed. All chiral auxiliaries used as alcohols or amines during synthesis were commercial samples. *cis*-2,3-Diphenylcyclopropane-1-carboxylic acid *trans*-2,3-diphenylcyclopropane-1-carboxylic acid were prepared by a literature procedure.[25]

Thermal reaction under the same reaction conditions (no irradiation) showed no isomerization, and the compounds were recovered with >95% mass balance.

Synthetic procedures and spectra data of all compounds (**1**−**24**) used in this study are provided as Supporting Information. The Supporting Information also contains HPLC/GC analysis conditions of the photoproducts.

Calculation of the Number of Supercages. Molecular formula of one unit cell of NaY (wet): $Na_{56}[(AlO_2)_{56}(SiO_2)_{136}]\cdot 250H_2O$; weight of 1 unit cell of NaY (wet) = [(56 × 22.99) + (56 × 59 + (136 × 60) + 250 × 18)] = 17 246 g mol^{-1}; weight of 1 unit cell of NaY (dry) = 12 746 g mol^{-1}. This implies 300 mg of NaY (wet) will have 222 mg of NaY (dry). The number of supercages[5] in 1 unit cell of NaY = 8. Molecular weight of 1 supercage for wet NaY = [12 746 g mol^{-1}/8] = 2155.75 g mol^{-1}. Molecular weight of 1 supercage for dry Na = [12 746 g mol^{-1}/8] = 1593.25 g mol^{-1}, Hence, the number of supercages in 300 mg of NaY (wet) = [0.3 g/2155.75 g mol^{-1}] = 1.39 × 10^{-4} mol; (or) number of supercages in 222 mg of NaY (dry) = [0.222 g/1593.25 g mol^{-1}] = 1.39 × 10^{-4} mol.

Calculating the Loading Level. For example, loading 3 mg of *cis*-**8** in 300 mg of NaY (wet) corresponds to 1 molecule in 15.7 supercages. As 3 mg of *cis*-**8** (molecular weight: 341 g mol^{-1}) = [3 mg/341 g mol^{-1}] = 8.8 × 10^{-6} mol. The number of supercages in 300 mg of NaY (wet) = [0.3 g/2155.75 g mol^{-1}] = 1.39 × 10^{-4} mol. Loading of 3 mg of *cis*-**8** in 300 mg of NaY (wet) = 1.39 × 10^{-4} mol/8.8 × 10^{-6} mol =15.7. Thus, the loading level of 3 mg of *cis*-**8** corresponds to a loading of 1 molecule in 15.7 supercages.

Calculation of Number of Cations. Molecular formula of one unit cell of NaY (wet): $Na_{56}[(AlO_2)_{56}(SiO_2)_{136}]\cdot 250H_2O$. Number of cations (alkali metal ions) = number of aluminum atoms = 56.

Photoisomerization in Solution. *cis*-2,3-Diphenylcyclopropane-1-carboxylic acid derivative (2−3 mg) was dissolved in 0.5 mL of dichloromethane in a quartz test tube followed by the addition of 15 mL of hexane. The test tube was stoppered with a rubber septum and wound with Parafilm. The solution was irradiated (unfiltered output from a 450 W medium-pressure mercury lamp) for 90 min, concentrated, and analyzed by GC/HPLC.

Photoisomerization Inside a Zeolite. *cis*-2,3-Diphenylcyclopropane-1-carboxylic acid derivative (2−3 mg) was dissolved in 0.5 mL of dichloromethane in a test tube. Hexane (15 mL) was added to the test tube and stirred. To the solution was added zeolite MY (M = Li$^+$, Na$^+$, K$^+$, Rb$^+$ and Cs$^+$; ∼300 mg) activated at 500 °C. The test tube was stoppered with a rubber septum, wound with Parafilm, and stirred for 8 h. The slurry was filtered and washed with hexane. Analysis of the filtrate (hexane solution) indicated that the diphenylcyclopropane derivative was completely incorporated inside the zeolite. The zeolite/substrate complex was dried in a vacuum (2 × 10^{-3} Torr) with heating at 60 °C for 8−10 h. The dried zeolite complex was transferred into a quartz test tube inside the drybox, and 10 mL of fresh dry hexane was added to the quartz tube. The test tube was stoppered with a rubber septum and wound with Parafilm. The slurry was irradiated (unfiltered output from a medium pressure of Hg lamp) for 90 min and filtered. Analysis of the hexane supernatant after irradiation did not show the presence of reactant/photoproducts. The reactant and the photoproducts were extracted from the zeolite by stirring with acetonitrile for 8−10 h. The acetonitrile extract was concentrated and analyzed by GC/HPLC.

Triplet-Sensitized Photoisomerization in Solution.

(a) Acetone Sensitization. *cis*-2,3-Diphenylcyclopropane-1-carboxylic acid derivative (2−3 mg) was dissolved in 12 mL of acetone in a test tube, stoppered, and wound with Parafilm. The solution was degassed with N_2 for 30 min and irradiated (unfiltered output from a 450 W medium-pressure mercury lamp) for 90 min. The solution was concentrated and analyzed by GC/HPLC.

(b) *p*-Methoxyacetophenone Sensitization. *cis*-2,3-Diphenylcyclopropane-1-carboxylic acid derivative (2−3 mg) and *p*-methoxyacetophenone (∼5 mg) were dissolved in 0.5 mL of dichloromethane in a test tube. Hexane (12 mL) was added, and the test tube was stoppered and wound with Parafilm. The solution was degassed with N_2 for 30 min and irradiated (unfiltered output from a 450 W medium-pressure mercury lamp) until the photostationary state was reached (∼48 h). The solution was concentrated and analyzed by GC/HPLC.

Sensitized Photoisomerization within Zeolites. 2,3-Diphenylcyclopropane-1-carboxylic acid derivative (2−3 mg) and the triplet sensitizer (20−25 mg) were dissolved in 0.5 mL of dichloromethane and 15 mL of hexane in a test tube and stirred. MY (M = Li$^+$, Na$^+$, K$^+$, Rb$^+$ and Cs$^+$) zeolite (∼300 mg) activated at 500 °C was added with stirring. The test tube was stoppered with a rubber septum and wound with Parafilm. The slurry was stirred for 12 h in a water bath kept at 55 °C, filtered, and washed thoroughly with fresh hexane (supernatant was analyzed for the presence of reactant/sensitizer). The zeolite was dried under high vacuum (2 × 10^{-3} Torr) at 60 °C for 12 h. The dried zeolite sample was transferred into a test tube inside a drybox, and fresh dry hexane was added. The test tube was stoppered with a rubber septum and wound with Parafilm. The slurry was degassed with N_2 for 30 min and then irradiated (unfiltered output from a 450W medium-pressure mercury lamp) as a hexane slurry under positive

(25) (a) Blatchford, J. K.; Orchin, M. *J. Org. Chem.* **1964**, *29*, 839. (b) D'Yakanov, I. A.; Komendantev, M. I.; Gui, F.-S.; Korichev, G. L. *J. Gen. Chem. USSR* **1962**, *32*, 928. (c) Applequist, D. E.; Gdanski, R. D. *J. Org. Chem.* **1981**, *46*, 2502. (d) Inoue, Y.; Yamasaki, N.; Shimoyama, H.; Tai, A. *J. Org. Chem.* **1993**, *58*, 1785−1793.

nitrogen pressure until the photostationary state (24−36 h), filtered, and washed again with fresh hexane. The supernatant was analyzed for the presence of reactant and photoproducts (reactant/photoproducts were not observed). The reactant and the photoproducts were extracted from the zeolite by stirring with acetonitrile. The extract was concentrated and analyzed by GC/HPLC.

Computational Methods

Binding Energies and Structures of Li^+-Bound *cis*- and *trans*-8, *cis*- and *trans*-9, *cis*-10, *cis*-11, and *cis*-18. Ab initio molecular orbital calculations using the Hartree−Fock as well as the hybrid Hartree−Fock density functional theory methods with B3LYP functional were carried out using the Gaussian98 suite of quantum chemical programs. The 3-21G and 6-31G* basis set, respectively, were used for HF and B3LYP calculations. Stationary points were characterized as true minima on the corresponding potential energy surfaces by performing frequency calculations with the "no Raman" option. For metal-bound structures, frequency calculations were done on representative Li^+-bound systems. These calculations does not include any explicit structural features of the zeolite framework. For structures *cis*-**10**, *cis*-**11**, and *cis*-**18**, calculations were done only at the HF/3-21G level.

Binding Energies and Structures of Li^+-Bound *cis*-8 and Its Transformation to *trans*-8-*RR* and *trans*-8-*SS*. The choice of starting geometries was primarily guided by the restricted rotation around the amide bond (as in *cis*-**8**, *cis*-**9**, etc.). Full-geometry optimization on cation-bound structures was performed on four basic conformers of *cis*-**8** and *cis*-**9** (Scheme 4), first at the HF/3-21G and subsequently at the B3LYP/6-31G* levels of theories. The binding affinities were evaluated using the "super system" approach and does not include basis set superposition error (BSSE) corrections. Binding affinities in each of the unique binding modes were determined on the basis of the optimized geometries of metal-ion-bound and metal-ion-free geometries for that conformation.

Acknowledgment. V.R. thanks the National Science Foundation for support of the research (CHE-9904187 and CHE-0212042) and Professor J. R. Scheffer and Dr. K. C. W. Chong for insightful discussions.

Supporting Information Available: Synthetic procedures and spectral data for compounds **1**−**19** and **22**−**24**, HPLC and GC analyses conditions for photoproducts from **1**−**24**, methods adopted to determine the absolute configuration of *trans*-**2**, and compilation of Cartesian coordinates and total energies for computed structures related to Figures 4−9. This material is available free of charge via the Internet at http://pubs.acs.org.

JO049365I